Journal of Chromatography A 1756 (2025) 466070

Contents lists available at ScienceDirect

Journal of Chromatography A

journal homepage: www.elsevier.com/locate/chroma

Implementation of ion exclusion chromatography for characterization of lithium ion battery materials

Stefan van Wickeren [a,1], Lukas Ihlbrock [a,1], Christoph Peschel [a], Simon Wiemers-Meyer [a], Martin Winter [a,b], Sascha Nowak [a,*]

[a] University of Münster, MEET Battery Research Center, Corrensstraße 46, 48149, Münster, Germany
[b] Helmholtz-Institute Münster, IMD-4, Forschungszentrum Jülich, Corrensstraße 46, 48149, Münster, Germany

ARTICLE INFO

Keywords:
Ion exclusion chromatography
Fluorine quantification
Lithium ion batteries
Fluoroethylene carbonate
Electrolyte decomposition
Solid electrolyte interphase

ABSTRACT

Inorganic compounds such as lithium fluoride (LiF) and lithium carbonate (Li_2CO_3) as well as weakly acidic lithium salts like lithium acetate ($LiCH_3CO_2$) or lithium formate ($LiHCO_2$) are reported decomposition products in lithium ion batteries (LIBs). The simultaneous analysis of these compounds is challenging due to the complex system consisting of conductive salt, organic carbonates, additives and their decomposition variety. Ion exclusion chromatography with conductivity detection (IEC-CD) seems to be predestinated for this analytical task due to its ability to separate and determine weakly acidic anions, which are the relevant species arising from lithium salts and electrolyte decomposition processes. One important chromatographic method to analyze ionic decomposition products is ion exchange chromatography (IC), which is currently a state-of-the-art (SOTA) technique for fluoride (F^-) quantification in LIBs. However, the calibration curve of F^- by IC hyphenated to a conductivity detection (CD) provides a small linear range for low concentrations and an analyte dependent retention shift occurs. IEC-CD represents a substantial upgrade in this respect and generated benefits for electrolyte analysis by an improved linear range for F^- (up to several 100 ppm). Furthermore, especially in complex samples, the IEC-CD method provides a more reliable chromatographic separation. In this study, IEC-CD is implemented to investigate decomposition pathways of fluor-releasing electrolyte additives such as fluoroethylene carbonate (FEC). The quantification of formate (HCO_2^-), acetate ($CH_3CO_2^-$) and carbonate (CO_3^{2-}) was also possible to gain deeper understanding of electrolyte additive decomposition in LIBs.

1. Introduction

Since their market implementation, lithium ion batteries (LIBs) have become integral part of our society and their success story has exploited new application areas such as electric vehicles, energy storage systems or aviation. With the increasing capacities in battery manufacturing and ongoing optimization of battery technology, the mobility sector has been spotted as perfect target for LIBs [1–3].

State-of-the-art (SOTA) LIBs provide the best compromise of long cycle life combined with high energy efficiency and energy density. The operating cell voltages (> 3.5 V) and decent specific gravimetric/volumetric energy densities on cell level (up to 260 Wh kg^{-1}/ 750 Wh L^{-1}) are much higher compared to other rechargeable battery systems resulting in superior driving range for electric vehicles [4–7].

A limitation of LIBs during operation and storage is the degradation of the cell components (aging), resulting in performance loss and a reduced cycle lifetime. In this regard, the LIB electrolyte stability represents one major aging aspect [8,9]. For instance, Heider *et al.* and Aurbach *et al.* showed a hydrolysis reaction of lithium hexafluorophosphate ($LiPF_6$) in organic solvents, whereby hydrogen fluoride (HF) is formed [10,11]. HF formation can lead to a rapid breakdown of the cell due to the dissolution of active material [12,13]. Furthermore, typical decomposition products are inorganic compounds such as lithium carbonate (Li_2CO_3) and lithium fluoride (LiF) as well as weakly acidic lithium salts like lithium acetate ($LiCH_3CO_2$) and lithium formate ($LiHCO_2$) that are reported as key components of the solid electrolyte interphase (SEI) [14–16]. Anyhow, the exact decomposition mechanisms of the electrolyte at the electrode interfaces are still unclear.

To evaluate the formation and occurrence of these compounds, robust and sensitive characterization techniques are required. One

* Corresponding author.
E-mail address: Sascha.nowak@uni-muenster.de (S. Nowak).
[1] both authors contributed equally

https://doi.org/10.1016/j.chroma.2025.466070
Received 21 February 2025; Received in revised form 7 May 2025; Accepted 18 May 2025
Available online 22 May 2025

important chromatographic method to analyze ionic decomposition products is ion exchange chromatography (IC) [17]. The determination of the above mentioned anions by IC suffers from poor linearity or retention is not possible, since these anions are used in the mobile phase. In contrast, IC with typical anion exchange phase is the method of choice to analyze typical conducting salts and anionic additives like $LiPF_6$, lithium difluoro phosphate ($LiPO_2F_2$), lithium bis(fluorosulfonyl)imide (LiFSI) or lithium bis(oxalato)borate (LiBOB).

Implementation of ion exclusion chromatography with conductivity detection (IEC-CD) is promising due to high selectivity to weakly acidic anions [18]. Exemplarily, IEC-CD is suitable for the investigation of electrochemically and thermally aged electrolytes. Since fluoride (F^-) determination is challenging or even impossible by using element specific analytical techniques such as inductively coupled plasma-mass spectrometry (ICP-MS) or X-ray fluorescence (XRF), IEC-CD is of even more interest. For analyzing battery electrolytes, IEC-CD has not yet been applied, although F^- as well as carbonate (CO_3^{2-}) are key compounds present in SOTA LIBs.

2. Experimental part

2.1. Chemicals

All chemicals were analytical grade unless otherwise stated. Acetonitrile (ACN), ethanol (EtOH) and ethyl acetate (EtAc) were purchased from VWR (Germany). LiFSI were used from Lonza Group (Switzerland, 99 %). Chloride standard, fluoride standard, FEC, formic acid (HCOOH, 98 %), methanol and phosphate standard were provided by Sigma-Aldrich (USA) and diethyl carbonate (DEC), dimethyl carbonate (DMC), dimethylformamide (DMF), dimethylsulfoxide (DMSO), ethylene carbonate (EC), ethyl methyl carbonate (EMC), sodium acetate ($NaCH_3COO$) and sodium carbonate (Na_2CO_3) were used from Merck (Germany). Lithium bis(trifluoromethanesulfonyl)imide (LiTFSI, Battery Grade) were purchased from TOB New Energy (China).

2.2. Cell assembly and electrochemical aging

Dry and sealed NMC622||graphite machine-made pouch cells were used from Li-FUN Technology (China) for thermal and electrochemical aging, which was performed on a battery and cell testing system (MACCOR, USA). Prior to filling, the cells were dried in a vacuum oven (Binder, Germany) at 60 °C for 12 h. The dried cells were filled with 750 µL of electrolyte and sealed with a GN—HS200V vacuum sealer (Gelon LIB, China) for 5 s at 165 °C and 83 kPa.

Prior to cell formation, the cells were rested for 10 h to ensure homogeneous electrolyte distribution in the cell. After that, the constant current formation was performed with two cycles in a voltage range of 3.0 V to 4.2 V and a charge/discharge current rate of 0.2 C.

2.3. Cell opening and sample processing

The discharged cells were opened in a glove box (MBraun, Germany) by cutting out the electrode stack with a ceramic scalpel and the electrodes were separated from each other. To obtain pure electrolyte, anode and separator were transferred into 50 mL tubes (VWR, USA) with a shortened 20 mL syringe housing and were centrifuged in a Mega Star 600R centrifuge (VWR, USA) for 20 min at 8000 rpm and 20 °C. For electrolyte analysis, the electrolytes were diluted volumetrically in dimethylsulfoxide (DMSO (1/20 (*v*/*v*)) but monitored gravimetrically and recalculated.

2.4. Ion exclusion chromatography-conductivity detection

Electrolyte measurements were carried out by means of IEC-CD. Therefore, an 850 Professional IC Anion-MCS system equipped with the Metrosep Organic Acids - 250/7.8 (Metrohm, Switzerland) column and 889 IC sample center were used. The column consists of a polystyrol/divinylbenzol copolymer basis with sulfonated modifications with a dimension of 250 mm length and 7.8 mm width. The suppressor was regenerated with 0.25 mmol L^{-1} lithium chloride [19]. The measurements were performed with an injection volume of 20 µL. A diluted sulfuric acid solution (0.5 mmol L^{-1}) was used as mobile phase and the optimized temperature was 30 °C. The detailed instrumental parameters for IEC-CD measurements are listed in Table 1.

2.5. Ion exchange chromatography-conductivity detection

The determination of the calibration curve of F^- for 1, 2, 5, 10, 20 and 50 ppm (see Fig. 2) and the solubility experiments of $LiPF_6$ and LiTFSI based electrolytes to determine the $LiPF_6$ and LiTFSI content were carried out by means of IC-CD. Therefore, an 850 Professional IC Anion-MCS system and 889 IC sample center (Metrohm, Switzerland) were used. A Metrosep A Supp 7- (250 × 4.0 mm), 5 µm; Metrohm) with a Metrosep A Supp 4/5 guard column was used for isocratic anion separation at 65 °C and a flow rate of 0.7 mL min^{-1} was applied [20,21]. The column material consists of a polyvinyl alcohol with quaternary ammonium modification. The parameters set for this separation technique are shown in Table 2.

3. Results & discussion

3.1. Method development and validation of ion exclusion chromatography

For sufficient separation, a 0.5 mmol L^{-1} sulfuric acid solution without an organic modifier was used as eluent, because 15 vol. % acetone resulted in a poor base signal and a solvent peak. The impacts of the flow rate and temperature were experimentally determined. A flow rate of 0.55 mL min^{-1} was the most suitable and is at the upper end (max. flow rate of 0.6 mL min^{-1}) of the range recommended by the column manufacturer [22]. Despite the high flow rate, a sufficient separation of the analytes under investigation was given. The temperature did not affect the separation of the components drastically, which is why all measurements were carried out at moderate 30 °C. Elevated temperatures prove less effective due to the extended equilibration time required for the IEC-CD and higher energy consumption of the IEC system. The IEC-CD measurements of a solution of F^-, formate (HCO_2^-), acetate ($CH_3CO_2^-$) and CO_3^{2-} in sulfuric acid are shown exemplarily for a flow rate of 0.3 mL min^{-1} and 0.55 mL min^{-1} at 30 °C (see Fig. 1).

IEC-CD analysis of the standard compounds resulted in baseline separated peaks (see S1 a). Peak assignment was performed by individual analysis of the four compounds. The 0.5 mmol L^{-1} sulfuric acid solution ensured a pH-value from approx. 3 and under these conditions HF exhibits the strongest dissociation rate ($pK_a = 3.18$) [23] and undergoes the least retention. Formic acid ($pK_a = 3.75$) [24] eluted with a retention time of approx. 12.5 min followed by acetic acid ($pK_a = 4.76$) [24]. Carbonic acid (H_2CO_3, $pK_a = 6.35$) [24] passed the column more slowly because of the lowest dissociation constant. The low degree of dissociation of H_2CO_3 facilitates a higher frequency of passage through the so-called Donnan membrane and enables increased interaction with the stationary phase. The charged Donnan membrane shields dissociated

Table 1
Overview of parameters set for IEC-CD.

IEC-Parameter	Settings
Eluent	0.5 mmol L^{-1} H_2SO_4
Injection volume	20 µL
Flow rate	0.55 mL min^{-1}
Pressure	3.3 MPa
Temperature	30 °C
Detection	Conductivity

Table 2
Overview of parameters set for IC-CD.

IC-Parameter	Settings
Eluent	3.6 mM Na_2CO_3, 3.4 mM $NaHCO_3$, 42 Vol. % ACN
Injection volume	20 µL
Flow rate	0.7 mL min^{-1}
Pressure	10.5 MPa
Temperature	65 °C
Detection	Conductivity

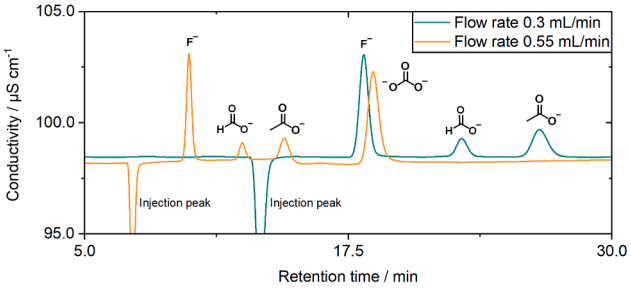

Fig. 1. Zoomed and overlaid chromatograms for the separation of a solution of F^- (10 ppm), HCO_2^- (5 ppm), $CH_3CO_2^-$ (15 ppm) and CO_3^{2-} (150 ppm) in sulfuric acid for a flow rate of 0.3 mL min^{-1} (light blue) and 0.55 mL min^{-1} (orange). CO_3^{2-} eluted at a flow rate of 0.3 mL min^{-1} after 30 min and was therefore not detected.

molecules, while uncharged analytes can cross the membrane. The individual measurements of the acids confirmed the retention times expected from the pK_a-values (see S1 b).

Further experiments were performed to measure other ionic species commonly found in LIBs like hexafluorophosphate (PF_6^-), phosphate (PO_4^{3-}), bis(trifluoromethanesulfonyl)imide ($TFSI^-$), bis(flurorosulfonyl) imide (FSI^-) and chloride (Cl^-). Notably, PF_6^-, $TFSI^-$ and FSI^- hold noteworthy interest due to their utilization as co-conducting salt anions and their substantial presence in high concentrations. PO_4^{3-} can be formed due to the hydrolysis of $LiPF_6$ with water as the final product [25]. Cl^- may occur as contamination from synthesis. As expected, the dissociation of PF_6^-, PO_4^{3-}, $TFSI^-$, FSI^- and Cl^- was too high and therefore they were not retained at the stationary phase. The target analytes underwent excellent and selective separation without any chromatographic interferences.

A notable limitation of IC-CD for F^- quantification is the narrow linear range for high concentrations and an analyte concentration dependent retention shift occurs as visualized in Fig. 2 a) and b).

The calibration curve of F^- obtained by IEC-CD provides a wider linear range as depicted in d). The calibration curve is shown for 1, 5, 10, 20, 40, 60, 80 and 100 ppm with a correlation coefficient of 0.999. All measurements were carried out with a threefold determination with high reproducibility. In comparison with IC-CD, the basic conductivity of IEC-CD is higher with approx. 96 - 100 µS cm^{-1}. In IC-CD, sodium bicarbonate was used as eluent and the suppressor consisted of an ion exchange column in its hydrogen form. The hydrogen exchange of the eluent formed CO_2 in water with a low conductivity. Moreover, a CO_2 suppressor was applied to further decrease background conductivity to <1 µS cm^{-1}. In IEC-CD, the suppressor was regenerated with lithium chloride (25 mmol L^{-1}) and the Li^+ ions exchanged with the H^+ ions forming a less, but still conductive Li^+ form. The IEC-CD represents a substantial upgrade for the linear range, because no slope decreasing for higher concentrations of F^- could be detected. Samples containing > 300 ppm F^- are still in the linear range. In addition to the improved linear range for quantification, more stable retention behavior was achieved. In Fig. 2 a), a clear retention shift to shorter retention times for high concentrations can be observed by IC-CD, which no longer occurs in the IEC-CD measurements (see Fig. 2 c)). Especially in complex samples, the IEC-CD method provides a more reliable identification of the analytes based on the retention times. However, an asymmetric peak shape for high concentrations is noticeable. Fronting was evident in the peaks corresponding to higher concentrations, a phenomenon frequently attributed to column overloading with analytes. Additionally, the calibration curve could be consistently applied over an extended duration owing to the resilient nature of the detection method.

In S2 and S3, the overlaid chromatograms and the calibration curve for 1, 5, 10, 25, 50, 75 and 100 ppm are depicted for HCO_2^- and $CH_3CO_2^-$ measured by IEC-CD. These compounds also showed a wide linear working range with a correlation coefficient of 0.999, enabling precise quantification of HCO_2^- and $CH_3CO_2^-$. One advantage compared to F^- is the more symmetrical peak shape even at increased concentrations.

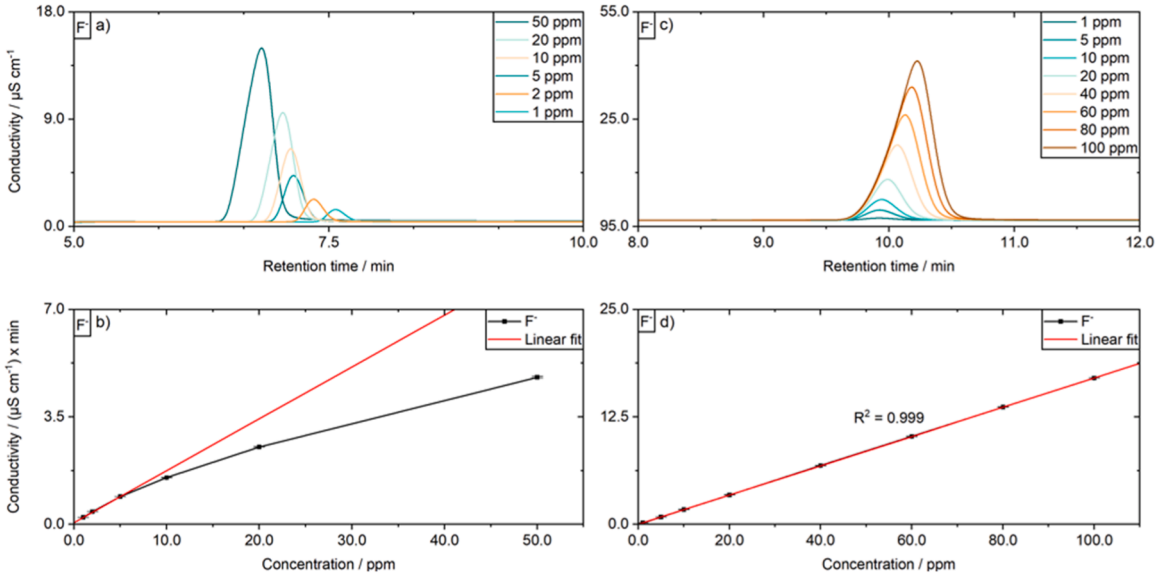

Fig. 2. a), b): Zoomed IC-CD chromatograms and calibration curve for F^- for 1, 2, 5, 10, 20 and 50 ppm. The linear regression fit was plotted for 1, 2 and 5 ppm. The IC-CD method presents the current SOTA quantification of F^- in the context of LIBs [20,26] c), d): Zoomed and overlaid chromatograms for the determination of the calibration curve for F^- measured by IEC-CD (c)). The calibration curve for F^- is shown for 1, 5, 10, 20, 40, 60, 80 and 100 ppm (d)). The measurements were carried out in water and a threefold determination with high reproducibility was obtained.

The calibration curve of CO_3^{2-} was determined within the range of 10 to 400 ppm as shown in S4, yielding a high correlation coefficient of 0.999. Slight conductivity deviations of the calibration curve measurements were observed possibly attributed to absorption of CO_2 into the solvent medium resulting in increased CO_3^{2-} content over time. Furthermore, the calibration curves duration of applicability was comparatively shorter than that of F^-, HCO_2^- and $CH_3CO_2^-$ and had to be recalibrated regularly. Nevertheless, a broad linear range was obtained, allowing CO_3^{2-}quantification *via* IEC-CD in comparison to IC-CD.

The limits of detection (LODs) were experimentally determined for F^-, CO_3^{2-}, HCO_2^- and $CH_3CO_2^-$ (listed in Table 3). For all measurements the samples were diluted in water. All calibration levels were measured three times and if the calibration level did not match the linear detection range, they were not considered. The limits of quantification (LOQ) were determined according to Eq. (1) based on the slope of the calibration curve and the standard error of the regression (SD[x/y]). F^- has the lowest LOD (0.09 ppm), followed by HCO_2^- and $CH_3CO_2^-$ (LOD: 0.25 ppm). CO_3^{2-} shows a LOD of 1.0 ppm.

$$\mathrm{LOQ} = \mathrm{LOD} \cdot \frac{10}{3} \;\Big|\; \mathrm{LOD} = 3\ \mathrm{SD}\frac{[y/x]}{\mathrm{slope}};\ \mathrm{LOQ} = 10\ \mathrm{SD}\frac{[y/x]}{\mathrm{slope}} \qquad (1)$$

The developed IEC method shows comparable LODs to F^- selective analytical techniques (see Table 4). An indirect IC-ICP-MS methodology introduced by Bayón *et al.* comprises lowest LOD of $1 \cdot 10^{-4}$ ppm F^- [27]. This method bases on formation of aluminum monofluoride (AlF^{2+}) in excess of Al^{3+} cations analyzed by cation chromatography hyphenated to ICP-MS. The detection is realized by monitoring aluminum at mass to charge (m/z) 27. Anyhow, a complex instrumental setup with different hyphenation linkages is required. Furthermore, a thermal treatment for quantitative formation of AlF^{2+} complex is essential, which can result in artefacts by temperature-sensitive compounds in the electrolyte.

IC-CD shows lower LODs than IEC-CD. However, drawbacks of IC are already discussed above. Moreover, coelution of decomposition products of $LiPF_6$-based electrolytes can take place in battery application without usage of complex two-dimensional chromatographic systems [28].

In addition, F^- selective electrodes (FSE) are challenging for F^- quantification in batteries. While the low pH-value of the electrolyte should overcome cross-selectivity to hydroxide anions, metal ions from the cathode or current collector can interfere (Fe^{2+}/Fe^{3+}or Al^{3+}). Furthermore, the electrode response depends on the F^- activity, not concentration. This activity varies, among other things, on the total ion concentration of the sample. Unfortunately, battery electrolytes contain high concentrations of the ionic conductive salt, which can lead to misquantification [29]. Due to electrode size, only high sample volumes are measurable by FSE (roughly 10 mL sample). Anyhow, the extraction efficiency of battery electrolytes is limited, and it is hard to gain higher amounts of electrolytes from end-of-life batteries.

Capillary electrophoresis (CE) methodologies are limited to their strong dependencies on matrix effects. Especially, high ionic strength (conductive salt) and organic compounds (carbonates) can affect the electric osmotic flow - the key separation driver of CE.

The shown IEC-CD method comprises different advantages compared to SOTA analytics of F^-. Especially, high selectivity not only to F^-, but also to HCO_2^-, $CH_3CO_2^-$ and $CO3^{2-}$ is promising. Easy instrumental setup, low-cost eluent/regenerant and low-temperature separation make IEC to a cost competitive alternative for battery electrolytes. The discrimination of high-concentrated matrix components (conductive salt, compounds with low pK_a and uncharged organic components) due to functionality of the Donnan membrane enables analysis of low-concentrated, weakly acidic electrolyte decomposition products. IEC is the first analytical method for simultaneous quantification of F^-, HCO_2^-, $CH_3CO_2^-$ and CO_3^{2-} in battery applications. In the next chapter, exemplarily applications for battery electrolyte analysis are shown.

Table 3
List of LODs and LOQs of F^-, HCO_2^-, $CH_3CO_2^-$ and CO_3^{2-}.

Analyte	LOD / ppm	LOQ / ppm
F^-	$9 \cdot 10^{-2}$	$3 \cdot 10^{-1}$
CO_3^{2-}	1.0	3.33
HCO_2^-	$2.5 \cdot 10^{-1}$	$8.3 \cdot 10^{-1}$
$CH_3CO_2^-$	$2.5 \cdot 10^{-1}$	$8.3 \cdot 10^{-1}$

Table 4
Comparison of SOTA analytical techniques for F^- quantification.

Method	LOD (F^- / ppm)	Reference
IEC	$9 \cdot 10^{-2}$	This work
CE	$9 \cdot 10^{-1}$	Pyschik *et al.*[30]
IC	$1 \cdot 10^{-2}$	Kumar *et al.*[31]
FSE	$3 \cdot 10^{-2}$	Chan *et al.*[32]
IC-ICP-MS	$1 \cdot 10^{-4}$	Bayón *et al.*[27]

3.2. Application of ion exclusion chromatography for electrolyte measurements

Besides the IEC-CD method development, the aim of this work was also the implementation of IEC-CD to study electrochemically and thermally aged electrolytes. Therefore, lithium bis(trifluoromethanesulfonyl)imide (LiTFSI) based electrolytes were used with ethylene carbonate (EC)/ diethyl carbonate (DEC) (3:7 wt. %, $EL_{LiTFSI+EC/DEC}$) and with additional FEC as an additive ($EL_{LiTFSI+EC/DEC+FEC}$). Fluorine-containing additives are applied in LIB electrolytes for several years because of the presumed formation of a highly fluorinated SEI due to reductive decomposition improving electrochemical performance [33]. For electrolyte additive studies regarding their F^- formation after decomposition, $LiPF_6$ can interfere the expressiveness of the data due to hydrolysis to HF and equilibrium with LiF. Therefore alternative, more stable salts such as LiTFSI were considered in this research. Electrochemical and thermal stability experiments were performed to exclude F^- release from the conductive salt. Furthermore, one aim of this research was to quantify additional weakly ionizable species like HCO_2^-, $CH_3CO_2^-$ and CO_3^{2-} in electrochemically and thermally aged electrolytes.

For qualitative investigations of the electrolyte the choice of solvent is crucial to exclude artefact formation after aging or ghost peak occurrence. As depicted in Fig. 3 a), the pure solvent blanks of H_2O, dimethyl sulfoxide (DMSO), ethanol (EtOH), methanol (MeOH), dimethyl carbonate (DMC), dimethylformamide (DMF) and acetonitrile (ACN) were measured. As visualized, just H_2O and DMSO were suitable for the simultaneous determination of F^-, HCO_2^-, $CH_3CO_2^-$ and CO_3^{2-} due to baseline instability of the other tested solvents.

For stability investigations of LiTFSI, the pristine electrolyte of $EL_{LiTFSI+EC/DEC+FEC}$ was diluted in different solvents and the LiTFSI concentration was measured by IC-CD. The measurements indicated the highest stability and the best recovery rate of LiTFSI in DMSO (see Fig. 3 b)).

To examine the stability of FEC in various solvents approx. 10 mg of FEC were dissolved in 1 mL of each solvent and were incubated 12 h at room temperature (see Fig. 3 c)). For the measurements, the samples were further diluted. As a result, FEC is unstable towards polar protic solvents such as MeOH, EtOH and especially H_2O. In the solutions of DMSO, ACN and DMC the F^- content was < LOD (0.09 ppm). Overall, the results showed that DMSO is the most suitable solvent for electrolyte analysis by means of IEC-CD. LiTFSI and the fluorine containing additive FEC are stable and did not provide any further F^- content through decomposition that could interfere the measurements. Consequently, further electrolyte measurements were carried out in DMSO. Nevertheless, it should be mentioned that the focus in the choice of the solvent was directed on simultaneous quantification of F^-, HCO_2^-, $CH_3CO_2^-$ and CO_3^{2-}.

For the aged electrolyte measurements, the LiTFSI based electrolytes

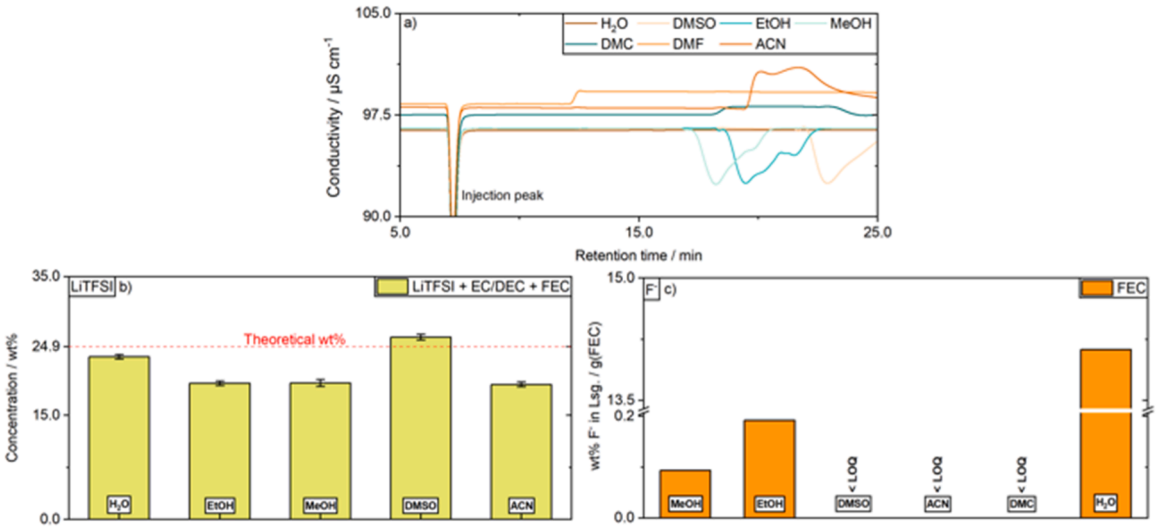

Fig. 3. a) Zoomed and overlaid chromatograms for the comparison of pure solvent blanks (H_2O: brown, DMSO: yellow, EtOH: blue, MeOH: light blue, DMC: dark blue, DMF: orange, ACN: light brown). b) The pristine electrolyte ($EL_{LiTFSI+EC/DEC+FEC}$) was solved in different solvents and the LiTFSI content was measured by IC-CD. The theoretical concentration is plotted at 24.9 wt %. c) The stability of FEC in MeOH, EtOH, DMSO, ACN, DMC and H_2O are depicted due to the determination of the F^- content by IEC-CD.

after cell formation at 20 °C and 60 °C were considered. For each aged electrolyte, three multi-layer pouch cells were built and formed at 20 °C and 60 °C and a twofold determination was carried out. Besides F^-, also HCO_2^-, $CH_3CO_2^-$ and CO_3^{2-} were quantified. In Fig. 4, the F^- contents of pristine and aged LiTFSI based electrolytes are depicted as a bar chart.

In contrast to the pristine electrolytes, no F^- content (< LOQ (0.3 ppm)) was found in the at 20 °C electrochemically formed $EL_{LiTFSI+EC/DEC}$. Thus, the aged electrolyte was perfectly suited to investigate the F^- content caused by fluorine containing additives such as FEC after electrochemical aging. It was concluded that the determined F^- content in $EL_{LiTFSI+EC/DEC+FEC}$ was formed exclusively by the corresponding additive [34,35]. Furthermore, Fig. 4 showed the F^- concentrations of $EL_{LiTFSI+EC/DEC}$ and with additional FEC for electrochemical formed cells at 60 °C. As visualized, due to the temperature increase to 60 °C during the formation process, F^- was detected for $EL_{LiTFSI+EC/DEC}$. In literature, low temperature decomposition of LiTFSI was associated to the release of trapped HF acid as residue from synthesis. Lu *et al.* described HF generation of pristine LiTFSI already at 36 °C via thermogravimetric analysis (TGA). However, only low amounts of HF were detected [36]. Initial F^- content in pristine electrolyte can be also caused by storage at slightly elevated temperatures. In general, electrolyte suppliers determine the F^- content to < 20 ppm.

Moreover, Krämer *et al.* explained a correlation of anodic aluminum

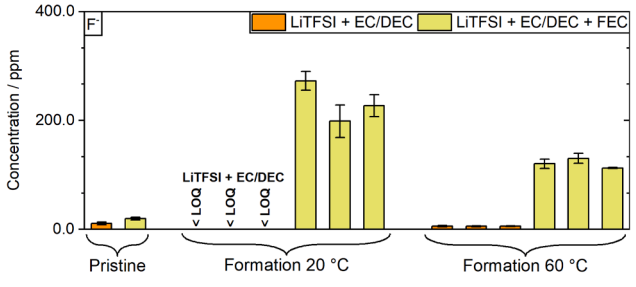

Fig. 4. Bar chart of the F^- contents of pristine and aged LiTFSI based electrolytes (formed at 20 °C and 60 °C) measured by IEC-CD. The pristine electrolyte measurements were carried out with a threefold determination. Three bars are shown for each aged electrolyte, corresponding to three different pouch cells. For each aged electrolyte, the mean value of the F^- content was calculated from a twofold determination ($EL_{LiTFSI+EC/DEC+FEC}$: light green, $EL_{LiTFSI+EC/DEC}$: orange).

current collector with electrolyte decomposition in carbonate-based electrolytes. Due to lack of passivating conductive salt or additives, aluminum can be dissolved into the electrolyte, but also further faradaic, parasitic reactions take place. Applying a constant voltage to LiTFSI based electrolytes leads to an increased F^- concentration during electrochemical oxidation process at the aluminum electrode [37].

Furthermore, reductive LiTFSI degradation is described at the interface of graphite and electrolyte. This LiTFSI based SEI consists among others of LiF and can result in increased F^- concentration in the electrolyte [38].

With additional FEC, the temperature change had exactly the opposite effect on the F^- concentration. It was also noticeable that the concentrations in the three individual electrolytes are more reproducible than for the formation process at 20 °C.

In literature, FEC is described as additive with superior SEI film-forming abilities due to ring-opening reaction at reductive surfaces and further LiF release as stable building block of the SEI. This LiF-rich SEI is particularly resistant to re-dissolution of SEI species in the electrolyte. The newly developed IEC analysis of the electrolyte delivers first correlation of dissolved F^- species exclusively formed by FEC. Besides the formation of stable immobile LiF in the SEI, FEC is causing F^- release into the electrolyte in form of LiF and HF [39,40].

Anyhow, it has to be stated, that the F^- content in the electrolyte is relatively small. The major amount of electrolyte decomposition products precipitates on the negative electrode. The lower F^- content at 60 °C formation temperature can be assigned to a more stable SEI or better kinetic decomposition behavior [41].

In contrast to the pristine electrolytes, HCO_2^- was quantified in the aged electrolytes formed at 20 °C and 60 °C (see Fig. 5), indicating that HCO_2^- is formed by electrochemical processes [16]. $LiHCO_2$ can be formed through the reaction of CO_2 radicals with protonic impurities such as HF [16]. As for F^-, in the absence of an additive, the concentration of HCO_2^- in the electrolyte was temperature-dependent. The concentration increased meaningfully with raising temperature. In the FEC containing electrolyte, variations in temperature did not lead to visible changes of the HCO_2^-content.

Similar to the determined F^- and HCO_2^- concentrations, the $CH_3CO_2^-$ content increased with a raising temperature of the formation process for $EL_{LiTFSI+EC/DEC}$ (see Fig. 5). For the FEC containing electrolyte, the concentration of $CH_3CO_2^-$ did not change notably with temperature. In general, the $CH_3CO_2^-$concentration was in a similar range for pristine and

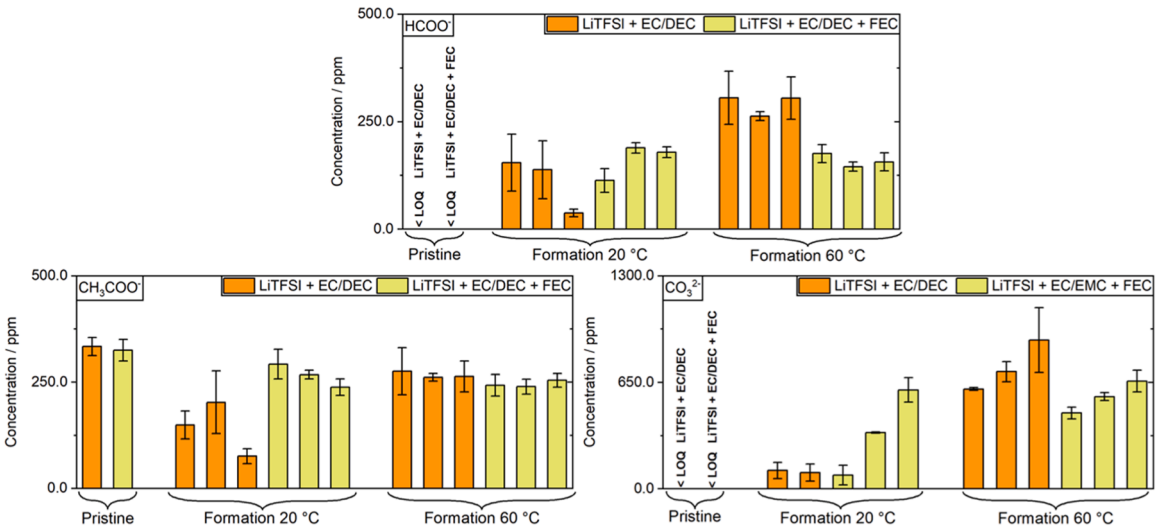

Fig. 5. Bar chart of the $HCOO^-$ (upper), CH_3COO^- (lower, left) and $CO3^{2-}$ (lower, right) content of pristine and aged electrolytes (formed at 20 °C and 60 °C) measured by IEC-CD. The pristine electrolyte measurements were carried out with a threefold determination. Three bars are shown for each aged electrolyte, corresponding to three different pouch cells. For each aged electrolyte, the mean value of the analyte content was calculated from a twofold determination ($EL_{LiTFSI+EC/DEC+FEC}$: light green, $EL_{LiTFSI+EC/DEC}$: orange).

aged electrolytes. Michan *et al.* presumed a $LiCH_3CO_2$ formation due to reactivity of alkoxy species with air. The alkoxy species are likely resulting from DMC and EC reactions [42].

In addition to F^-, HCO_2^- and $CH_3CO_2^-$, the quantification of CO_3^{2-} was also possible by means of IEC-CD. While no CO_3^{2-} was detected in the pristine electrolytes, it was also formed during formation (Fig. 5). One presumed formation of Li_2CO_3 involves the ring opening of EC [43]. Furthermore, formed semi-carbonates are reactive towards acids, water and CO_2. Therefore, Li_2CO_3 can be formed in situ during formation process. In addition, building of Li_2CO_3 artefacts during sample preparation or species separation cannot be excluded.

For the FEC containing electrolyte formed at 20 °C more F^-, HCO_2^-, $CH_3CO_2^-$ and CO_3^{2-} were detected than without additional FEC. The formation process at 60 °C led to reduced levels of HCO_2^- and CO_3^{2-} in the presence of FEC. However, $CH_3CO_2^-$ concentrations remained consistent across both formations. High temperature formation leads to a more effective and stable SEI. Therefore, the indirect SEI characterization *via* electrolyte analytics is challenging due to trapped species inside the SEI. Anyhow, insights into reductive decomposition pathways of the electrolyte and investigations of soluble SEI species can be performed *via* IEC-CD.

4. Conclusion

The understanding of electrode - electrolyte interphases regarding their formation, composition and stability is crucial for advanced cell chemistry designs for future LIBs. Powerful analytics are inevitable to effectively understand battery aging and performance. Thus, great efforts in the development of new analytical techniques have been made since their implementation.

This paper includes the method development and validation of a new IEC-CD and the ensuing application in LIB electrolyte characterization. The determination of F^- by IEC-CD offers great advantages over SOTA IC-CD method and can generate benefits for electrolyte analysis by an improved linear range with a LOD of 0.09 ppm. No retention shifts occurred by IEC-CD in contrast to IC-CD, which made the identification of the analytes based on the retention time much more reliable. Furthermore, simultaneous determination of weakly acids (HCO_2^-, $CH_3CO_2^-$ and CO_3^{2-}) was successfully applied.

This work provides evidence of the usefulness of the IEC-CD method as an analytical tool for electrolyte characterization. Besides a practical analysis, guideline (method parameter, solvent choice), the design of electrolyte composition and testing conditions were selected to evaluate the impact of the film-forming additive FEC on electrolyte decomposition reactions. A successful simultaneous determination of F^-, HCO_2^-, $CH_3CO_2^-$ and CO_3^{2-} in organic carbonate-based electrolytes was implemented. The effects of FEC and different formation temperatures on the electrolyte decomposition during film formation were investigated. IEC-CD could be a powerful and complementary tool in the diverse toolbox of chromatographic techniques for electrolyte studies.

CRediT authorship contribution statement

Stefan van Wickeren: Writing – review & editing, Writing – original draft, Visualization, Validation, Project administration, Methodology, Investigation, Formal analysis, Conceptualization. **Lukas Ihlbrock:** Writing – original draft, Validation, Methodology, Investigation, Formal analysis, Conceptualization. **Christoph Peschel:** Writing – review & editing, Conceptualization. **Simon Wiemers-Meyer:** Writing – review & editing, Supervision, Funding acquisition. **Martin Winter:** Writing – review & editing, Supervision, Funding acquisition. **Sascha Nowak:** Writing – review & editing, Supervision, Funding acquisition.

Declaration of competing interest

The authors declare that they have no known competing financial interests or personal relationships that could have appeared to influence the work reported in this paper.

Acknowledgement

The authors thank the German Federal Ministry of Education and Research (BMBF) for funding the project Cell-Fill (Grant number 03XP0237C).

Data availability

Data will be made available on request.

References

[1] T. Chen, Y. Jin, H. Lv, A. Yang, M. Liu, B. Chen, Y. Xie, Q. Chen, Applications of lithium-ion batteries in grid-scale energy storage systems, Trans. Tianjin Univ 26 (3) (2020) 208–217, https://doi.org/10.1007/s12209-020-00236-w.

[2] G.E. Blomgren, The development and future of lithium ion batteries, J. Electrochem. Soc 164 (1) (2017) A5019–A5025, https://doi.org/10.1149/2.0251701jes.

[3] T.P. Barrera, J.R. Bond, M. Bradley, R. Gitzendanner, E.C. Darcy, M. Armstrong, C.-Y. Wang, Next-generation aviation Li-ion battery technologies—Enabling electrified aircraft, Electrochem. Soc. Interface 31 (3) (2022) 69–74, https://doi.org/10.1149/2.F10223IF.

[4] P. Meister, H. Jia, J. Li, R. Kloepsch, M. Winter, T. Placke, Best practice: performance and cost evaluation of lithium ion battery active materials with special emphasis on energy efficiency, Chem. Mater 28 (20) (2016) 7203–7217, https://doi.org/10.1021/acs.chemmater.6b02895.

[5] P. Bieker, M. Winter, Lithium-Ionen-Technologie und was danach kommen könnte, Chem. Unserer Zeit 50 (3) (2016) 172–186, https://doi.org/10.1002/ciuz.201600745.

[6] J. Betz, G. Bieker, P. Meister, T. Placke, M. Winter, R. Schmuch, Theoretical versus practical energy: a plea for more transparency in the energy calculation of different rechargeable battery systems, Adv. Energy Mater. 9 (6) (2019) 1803170, https://doi.org/10.1002/aenm.201803170.

[7] R. Schmuch, R. Wagner, G. Hörpel, T. Placke, M. Winter, Performance and cost of materials for lithium-based rechargeable automotive batteries, Nat. Energy 3 (4) (2018) 267–278, https://doi.org/10.1038/s41560-018-0107-2.

[8] S. Nowak, M. Winter, Review—Chemical analysis for a better understanding of aging and degradation mechanisms of non-aqueous electrolytes for lithium ion batteries: method development, application and lessons learned, J. Electrochem. Soc 162 (14) (2015) A2500–A2508, https://doi.org/10.1149/2.0121514jes.

[9] J. Vetter, P. Novák, M.R. Wagner, C. Veit, K.-C. Möller, J.O. Besenhard, M. Winter, M. Wohlfahrt-Mehrens, C. Vogler, A. Hammouche, Ageing mechanisms in lithium-ion batteries, J. Power Sources 147 (1–2) (2005) 269–281, https://doi.org/10.1016/j.jpowsour.2005.01.006.

[10] U. Heider, R. Oesten, M. Jungnitz, Challenge in manufacturing electrolyte solutions for lithium and lithium ion batteries quality control and minimizing contamination level, J. Power Sources 81-82 (1999) 119–122, https://doi.org/10.1016/S0378-7753(99)00142-1.

[11] D. Aurbach, A. Zaban, Y. Ein-Eli, I. Weissman, O. Chusid, B. Markovsky, M. Levi, E. Levi, A. Schechter, E. Granot, Recent studies on the correlation between surface chemistry, morphology, three-dimensional structures and performance of Li and Li-C intercalation anodes in several important electrolyte systems, J. Power Sources 68 (1) (1997) 91–98, https://doi.org/10.1016/S0378-7753(97)02575-5.

[12] M. Evertz, F. Horsthemke, J. Kasnatscheew, M. Börner, M. Winter, S. Nowak, Unraveling transition metal dissolution of Li1.04Ni1/3Co1/3Mn1/3O2 (NCM 111) in lithium ion full cells by using the total reflection X-ray fluorescence technique, J. Power Sources 329 (2016) 364–371, https://doi.org/10.1016/j.jpowsour.2016.08.099.

[13] D.R. Gallus, R. Schmitz, R. Wagner, B. Hoffmann, S. Nowak, I. Cekic-Laskovic, R. W. Schmitz, M. Winter, The influence of different conducting salts on the metal dissolution and capacity fading of NCM cathode material, Electrochim. Acta 134 (2014) 393–398, https://doi.org/10.1016/j.electacta.2014.04.091.

[14] E. Peled, S. Menkin, Review—SEI: past, present and future, J. Electrochem. Soc 164 (7) (2017) A1703–A1719, https://doi.org/10.1149/2.1441707jes.

[15] T. Kawamura, S. Okada, J. Yamaki, Decomposition reaction of LiPF6-based electrolytes for lithium ion cells, J. Power Sources 156 (2) (2006) 547–554, https://doi.org/10.1016/j.jpowsour.2005.05.084.

[16] K.U. Schwenke, S. Solchenbach, J. Demeaux, B.L. Lucht, H.A. Gasteiger, The impact of CO 2 evolved from VC and FEC during formation of graphite anodes in lithium-ion batteries, J. Electrochem. Soc 166 (10) (2019) A2035–A2047, https://doi.org/10.1149/2.0821910jes.

[17] Y. Stenzel, F. Horsthemke, M. Winter, S. Nowak, Chromatographic techniques in the research area of lithium ion batteries: current State-of-the-art, Separations 6 (2) (2019) 26, https://doi.org/10.3390/separations6020026.

[18] L. Zhou, H. Li, S. Ye, H. Tan, A new method for determination of fluoride ion in commodity tea by ion-exclusion chromatography, CyTA-J. Food 16 (1) (2018) 637–641, https://doi.org/10.1080/19476337.2018.1441188.

[19] Jensen. Dr.Detlef, *Grundlagen Der Ionenchromatographie:Modernste Trenntechnik*, Thermo Scientific (2013).

[20] V. Kraft, M. Grützke, W. Weber, M. Winter, S. Nowak, Ion chromatography electrospray ionization mass spectrometry method development and investigation of lithium hexafluorophosphate-based organic electrolytes and their thermal decomposition products, J. Chromatogr. A 1354 (2014) 92–100, https://doi.org/10.1016/j.chroma.2014.05.066.

[21] J. Henschel, F. Horsthemke, Y.P. Stenzel, M. Evertz, S. Girod, C. Lürenbaum, K. Kösters, S. Wiemers-Meyer, M. Winter, S. Nowak, Lithium ion battery electrolyte degradation of field-tested electric vehicle battery cells - A comprehensive analytical study, J. Power Sources 447 (2020) 227370, https://doi.org/10.1016/j.jpowsour.2019.227370.

[22] Metrohm. Säulenprogramm:Die Ganze *Welt der Ionenchromatographie*. https://www.metrohm.com/de_de/products/6/1005/61005200.html (accessed 2025-02-11). 2025.

[23] Riedel, Anorganische Chemie, de Gruyter, 2004.

[24] D.R. Lide, CRC Handbook of Chemistry and Physics, 85, CRC press, 2004.

[25] L. Terborg, S. Nowak, S. Passerini, M. Winter, U. Karst, P.R. Haddad, P. N. Nesterenko, Ion chromatographic determination of hydrolysis products of hexafluorophosphate salts in aqueous solution, Anal. Chim. Acta 714 (2012) 121–126, https://doi.org/10.1016/j.aca.2011.11.056.

[26] M. Stich, M. Göttlinger, M. Kurniawan, U. Schmidt, A. Bund, Hydrolysis of LiPF 6 in carbonate-based electrolytes for lithium-ion batteries and in aqueous Media, J. Phys. Chem. C 122 (16) (2018) 8836–8842, https://doi.org/10.1021/acs.jpcc.8b02080.

[27] M.M. Bayón, A. Rodríguez Garcia, J.I. García Alonso, A. Sanz-Medel, Indirect determination of trace amounts of fluoride in natural waters by ion chromatography: a comparison of on-line post-column fluorimetry and ICP-MS detectors, Analyst 124 (1) (1999) 27–31, https://doi.org/10.1039/A807079B.

[28] V. Kraft, M. Grützke, W. Weber, J. Menzel, S. Wiemers-Meyer, M. Winter, S. Nowak, Two-dimensional ion chromatography for the separation of ionic organophosphates generated in thermally decomposed lithium hexafluorophosphate-based lithium ion battery electrolytes, J. Chromatogr. A 2015 (1409) 201–209, https://doi.org/10.1016/j.chroma.2015.07.054.

[29] A. Wilken, V. Kraft, S. Girod, M. Winter, S. Nowak, A fluoride-selective electrode (Fse) for the quantification of fluoride in lithium-ion battery (Lib) electrolytes, Anal. Methods 8 (38) (2016) 6932–6940, https://doi.org/10.1039/C6AY02264B.

[30] M. Pyschik, M. Klein-Hitpaß, S. Girod, M. Winter, S. Nowak, Capillary electrophoresis with contactless conductivity detection for the quantification of fluoride in lithium ion battery electrolytes and in ionic liquids-A comparison to the results gained with a fluoride ion-selective electrode, Electrophoresis 38 (3–4) (2017) 533–539, https://doi.org/10.1002/elps.201600361.

[31] S.D. Kumar, G. Narayan, S. Hassarajani, Determination of anionic minerals in black and kombucha tea using ion chromatography, Food Chem. 111 (3) (2008) 784–788, https://doi.org/10.1016/j.foodchem.2008.05.012.

[32] L. Chan, A. Mehra, S. Saikat, P. Lynch, Human exposure assessment of fluoride from tea (Camellia sinensis L.): a UK based issue? Food Res. Int. 51 (2) (2013) 564–570, https://doi.org/10.1016/j.foodres.2013.01.025.

[33] N. Xu, J. Shi, G. Liu, X. Yang, J. Zheng, Z. Zhang, Y. Yang, Research progress of fluorine-containing electrolyte additives for lithium ion batteries, J. Power Sources Adv. 7 (2021) 100043, https://doi.org/10.1016/j.powera.2020.100043.

[34] T. Hou, G. Yang, N.N. Rajput, J. Self, S.-W. Park, J. Nanda, K.A. Persson, The influence of FEC on the solvation structure and reduction reaction of LiPF6/EC electrolytes and its implication for solid electrolyte interphase formation, Nano Ener. 64 (2019) 103881, https://doi.org/10.1016/j.nanoen.2019.103881.

[35] V. Winkler, T. Hanemann, M. Bruns, Comparative surface analysis study of the solid electrolyte interphase formation on graphite anodes in lithium-ion batteries depending on the electrolyte composition, Surf. Interface Anal. 49 (5) (2017) 361–369, https://doi.org/10.1002/sia.6139.

[36] Z. Lu, L. Yang, Y. Guo, Thermal behavior and decomposition kinetics of six electrolyte salts by thermal analysis, J. Power Sources. 156 (2) (2006) 555–559, https://doi.org/10.1016/j.jpowsour.2005.05.085.

[37] E. Krämer, T. Schedlbauer, B. Hoffmann, L. Terborg, S. Nowak, H.J. Gores, S. Passerini, M. Winter, Mechanism of anodic dissolution of the aluminum current collector in 1 M LiTFSI EC:DEC 3:7 in rechargeable lithium batteries, J. Electrochem. Soc 160 (2) (2013) A356–A360, https://doi.org/10.1149/2.081302jes.

[38] C. Xu, B. Sun, T. Gustafsson, K. Edström, D. Brandell, M. Hahlin, Interface layer formation in solid polymer electrolyte lithium batteries: an XPS study, J. Mater. Chem. A 2 (20) (2014) 7256–7264, https://doi.org/10.1039/C4TA00214H.

[39] R. Jung, M. Metzger, D. Haering, S. Solchenbach, C. Marino, N. Tsiouvaras, C. Stinner, H.A. Gasteiger, Consumption of fluoroethylene carbonate (FEC) on Si-C composite electrodes for Li-ion batteries, J. Electrochem. Soc 163 (8) (2016) A1705–A1716, https://doi.org/10.1149/2.0951608jes.

[40] Y. Okuno, K. Ushirogata, K. Sodeyama, Y. Tateyama, Decomposition of the fluoroethylene carbonate additive and the glue effect of lithium fluoride products for the solid electrolyte interphase: an ab initio study, Phys. Chem. Chem. Phys. 18 (12) (2016) 8643–8653, https://doi.org/10.1039/C5CP07583A.

[41] S.J. An, J. Li, C. Daniel, D. Mohanty, S. Nagpure, D.L. Wood, The state of understanding of the lithium-ion-battery graphite solid electrolyte interphase (SEI) and its relationship to formation cycling, Carbon. N Y. 105 (2016) 52–76, https://doi.org/10.1016/j.carbon.2016.04.008.

[42] A.L. Michan, B.S. Parimalam, M. Leskes, R.N. Kerber, T. Yoon, C.P. Grey, B. L. Lucht, Fluoroethylene carbonate and vinylene carbonate reduction: understanding lithium-ion battery electrolyte additives and solid electrolyte interphase formation, Chem. Mater 28 (22) (2016) 8149–8159, https://doi.org/10.1021/acs.chemmater.6b02282.

[43] S.S. Zhang, A review on electrolyte additives for lithium-ion batteries, J. Power Sources 162 (2) (2006) 1379–1394, https://doi.org/10.1016/j.jpowsour.2006.07.074.